



Anomalies of hypersound velocity and attenuation in ferroelectric tris-sarcosine calcium chloride (TSCC) for Brillouin small angle, right angle and backscattering
by Jin Tong Wang

A thesis submitted in partial fulfillment of the requirements for the degree of Doctor of Philosophy in
Physics
Montana State University
© Copyright by Jin Tong Wang (1986)

Abstract:

The Brillouin spectra of the ferroelectric Tris-Sarcosine Calcium Chloride crystal have been observed in small angle, right angle and backscattering. The smallest angle we have achieved is 7.48° . The frequency range we were working on is about 2 GHz to 32 GHz. Brillouin investigation in such large frequency range is significantly important. The anomalies of hypersound velocity and attenuation were obtained.

We are the first to calculate the polarization of the scattered light in a orthorhombic crystal like TSCC. We are quite successful in interpreting the anomalies of sound velocities and attenuation for the phonon along [001] by piezoelectric coupling and we are the first to interpret the anomalies of sound velocities and attenuation for phonons along the polar axis [010] by the small depolarization effect.

We are the first experimentally to prove the relation $T_c - T_m \propto \omega$ for [001] phonons and $T_c - T_m = \text{Constant}$ for [010] phonons.

We estimated the elementary relaxation time $T_0 = 5.25 \times 10^{-14}$ sec for [001] phonons and $T_0 = 8.24 \times 10^{-12}$ sec for [010] phonons.

ANOMALIES OF HYPERSOUND VELOCITY AND ATTENUATION IN
FERROELECTRIC TRIS-SARCOSINE CALCIUM CHLORIDE
(TSCC) FOR BRILLOUIN SMALL ANGLE, RIGHT
ANGLE AND BACKSCATTERING

by

Jin Tong Wang

A thesis submitted in partial fulfillment
of the requirements for the degree

of

Doctor of Philosophy

in

Physics

MONTANA STATE UNIVERSITY
Bozeman, Montana

July, 1986

MAIN LIB.
D378
W1855
Cop. 2

© 1987

JIN TONG WANG

All Rights Reserved

APPROVAL

of a thesis submitted by

Jin Tong Wang

This thesis has been read by each member of the thesis committee and has been found to be satisfactory regarding content, English usage, format, citations, bibliographic style, and consistency, and is ready for submission to the College of Graduate Studies.

July 25, 1986
Date

V. Hugo Schmidt
Chairperson,
Graduate committee

Approved for the Major Department

July 25, 1986
Date

[Signature]
Head, Major Department

Approved for the College of Graduate Studies

July 28, 1986
Date

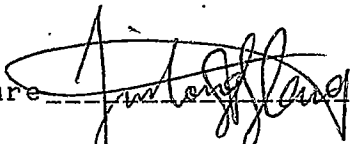
Henry Parsons
Graduate Dean

STATEMENT OF PERMISSION TO USE

In presenting this thesis in partial fulfillment of the requirements for a doctoral degree at Montana State University, I agree that the Library shall make it available to borrowers under rules of the Library. I further agree that copying of this thesis is allowable only for scholarly purposes, consistent with "fair use" as prescribed in the U. S. Copyright Law. Requests for extensive copying or reproduction of the thesis should be referred to University Microfilms International, 300 North Zeeb Road, Ann Arbor, Michigan 48106, to whom I have granted "the exclusive right to reproduce and distribute copies of the dissertation in and from microfilm and the right to reproduce and distribute by abstract in any format."

Signature _____

Date _____


July 25, 1986

ACKNOWLEDGEMENTS

The author wishes to thank the National Science Foundation, MONTS and the Physics Department of Montana State University for financial assistance and for providing the material and equipment used in this research. To his advisor, Dr. V. Hugo Schmidt, he is especially grateful for his very helpful discussion, instruction and for his help in personal things that bothered the author and his family very much. He especially thanks Dr. Tomi HIKITA for the fact that the author's experimental skills and elementary theoretical knowledge about Brillouin Scattering were learned from him. Dr. HIKITA taught unselfishly and useful suggestions for this research were given by him. It should be said Dr. HIKITA is the second advisor for Mr. Jin Tong Wang. He thanks Paul Schnackenberg and Paul Schuele for their experimental assistance. He thanks Professor Robert Gammon and Professor Herman Z. Cummins for their valuable discussion, Alfred Beldring for his efforts in repairing the laser optics and some other instruments and Professor George F. Tuthill and Professor Wm. M. Kinnersley for their help with the computer work.

TABLE OF CONTENTS

APPROVAL -----	ii
STATEMENT OF PERMISSION TO USE -----	iii
ACKNOWLEDGMENTS -----	iv
TABLE OF CONTENTS -----	v
LIST OF TABLES -----	vi
LIST OF FIGURES -----	vii
ABSTRACT -----	x
I. INTRODUCTION -----	1
II. THEORY OF BRILLOUIN SCATTERING IN ORTHORHOMBIC CRYSTAL -----	18
Introduction -----	18
The Spectrum of the Scattered Field -----	19
The Fluctuation $\delta\epsilon$ of the Dielectric Constant -----	36
Acoustic Modes in a Orthorhombic Crystal -----	41
The Polarization of the Scattered Light -----	51
III. EXPERIMENTAL EQUIPMENT AND TECHNIQUE -----	70
Introduction -----	70
General Description of the Apparatus -----	70
IV. EXPERIMENTAL RESULTS -----	93
Introduction -----	93
Data Analysis -----	93
The Brillouin Spectrum -----	97
Temperature Dependence of the Brillouin Shift (Phonon Frequency) and Line Width of Longitudinal Phonons in TSCC -----	103
The Sound Velocity Anomalies -----	128
Temperature Dependence of Dielectric Constant of TSCC -----	131
V. DISCUSSIONS -----	134
Introduction -----	134
The Crystal Structure of TSCC -----	135
The Phase Transition Category -----	140
Interpretation of Anomalies of Sound Velocity and Attenuation in TSCC -----	148
Conclusion -----	182
Suggestions for Future Work -----	184

LIST OF TABLES

Table		Page
1.	$q[010]$, $\theta=7.48^\circ$	101
2.	$q[010]$, $\theta=90^\circ$	103
3.	$q[010]$, $\theta=170^\circ$	105
4.	$q[001]$, $\theta=7.55^\circ$	107
5.	$q[001]$, $\theta=90^\circ$	109

LIST OF FIGURES

Figure	Page
1. Phase surface -----	3
2. Free energy and phase transition -----	4
3. Light scattering diagram -----	22
4. Refractive indicatrix -----	35
5. Wave vector and polarization for [010] phonons -----	49
6. Wave vector and polarization for [001] phonons -----	50
7. Experiment diagram -----	71
8. Light gathering -----	77
9. Computer operating FP -----	86
10. Cryostat -----	90
11. The refractive index -----	96
12. Brillouin spectrum -----	98
13. Temperature dependence of Brillouin shift of longitudinal [010] phonons for small angle scattering -----	110
14. Temperature dependence of Brillouin shift of longitudinal [010] phonons for right angle scattering -----	111
15. Temperature dependence of Brillouin shift of longitudinal [010] phonons for backscattering -----	112
16. Temperature dependence of Brillouin shift of longitudinal [001] phonon for small angle scattering -----	115

LIST OF FIGURES-CONTINUED

Figure	Page
17. Temperature dependence of Brillouin shift of longitudinal [001] phonon for right angle scattering -----	116
18. Temperature dependence of Brillouin shift of longitudinal [001] phonon for backscattering	118
19. Temperature dependence of Brillouin shift (.) and line width (.) of longitudinal [010] phonon for small angle scattering -----	119
20. Temperature dependence of Brillouin shift (.) and line width (.) of longitudinal [010] phonon for right angle scattering -----	121
21. Temperature dependence of Brillouin shift (.) and line width (.) of longitudinal [010] phonon for backscattering -----	122
22. Temperature dependence of Brillouin shift (.) and line width (.) of longitudinal [001] phonon for small angle scattering -----	123
23. Temperature dependence of Brillouin shift (.) and line width (.) of longitudinal [001] phonon for right angle scattering -----	125
24. Temperature dependence of Brillouin shift (.) and line width (.) of longitudinal [010] phonon for backscattering -----	116
25. Temperature dependences of sound velocities of longitudinal [010] phonons -----	129
26. Temperature dependences of sound velocities of longitudinal [001] phonons -----	130
27. Temperature dependence of the dielectric constant -----	133
28. The structure of TSCC viewed down its <u>a</u> axis	137

LIST OF FIGURES-CONTINUED

Figure	Page
29. Projection of half unit cell of TSCC along its <u>b</u> axis -----	138
30. Bond distances and angles -----	139
31. Psuedo-spin-phonon coupling -----	146
32. Temperature dependences of elastic constant for coupling linear and continuous transition	154
33. Temperature dependences of elastic constant for linear coupling in the strain but quadratic in order parameter -----	159
34. Relation of $T_c - T_n$ vs frequency for [001] phonons -----	169
35. Relation of $T_c - T_n$ vs frequency for [010] phonons -----	175
36. Phase diagram of TSCC -----	189

ABSTRACT

The Brillouin spectra of the ferroelectric Tris-Sarcosine Calcium Chloride crystal have been observed in small angle, right angle and backscattering. The smallest angle we have achieved is 7.48° . The frequency range we were working on is about 2 GHz to 32 GHz. Brillouin investigation in such large frequency range is significantly important. The anomalies of hypersound velocity and attenuation were obtained.

We are the first to calculate the polarization of the scattered light in a orthorhombic crystal like TSCC. We are quite successful in interpreting the anomalies of sound velocities and attenuation for the phonon along [001] by piezoelectric coupling and we are the first to interpret the anomalies of sound velocities and attenuation for phonons along the polar axis [010] by the small depolarization effect.

We are the first experimentally to prove the relation $T_c - T_m \propto \Omega$ for [001] phonons and $T_c - T_m = \text{constant}$ for [010] phonons.

We estimated the elementary relaxation time $\tau_0 = 5.25 \times 10^{-14}$ sec for [001] phonons and $\tau_0 = 8.24 \times 10^{-12}$ sec for [010] phonons.

CHAPTER I

INTRODUCTION

The study of phase transitions both theoretically and experimentally has found widespread interest during the past few years. Two main aspects make this subject so attractive: the many-particle or cooperative nature of these phenomena and the hypothesis of universality. It stands to reason that the field of phase transitions and critical phenomena has experienced a period of extremely rapid growth during the last two decades, both in the application of new experimental techniques and in the development of new theoretical approaches.¹

A given assembly of atoms and molecules may be homogeneous or inhomogeneous. The homogeneous parts of such an assembly, called phases, are characterized by thermodynamic properties like volume, pressure, temperature, and energy. An isolated phase is stable only when its free energy is a minimum for the specified thermodynamic conditions.

As to thermodynamic considerations, the classical

Clapeyron equation satisfactorily predicts the features of first-order phase transitions involving discontinuous changes in the first derivatives of the Gibbs free energy such as entropy and volume shown in Fig. 1. Unlike the case of first-order transition, where the free energy surfaces, $G(p, T)$, of the two phases intersect sharply at the transition temperature, it is difficult to visualize the nature of the free energy surfaces in second or higher-order transitions. In second-order transitions, where changes in heat capacity as well as compressibility and thermal expansivity are noticed at the transition, Landau made a momentous contribution to our understanding of phase transitions by expanding the free energy in terms of long-range order parameters Q ; Q decreases with an increase of temperature and goes to zero at the transition temperature. The concept of an order parameter today provides a very general way of examining phase transitions.²

The idea of phase transitions and spontaneous symmetry breaking has been widely used in physics since the 1930's (Landau 1937). Its application has been significant in both elementary particle physics, and for structural transitions, where it is described (Cochran, 1960, 1961) by the collapse of the energy of an optical phonon, i. e., "soft mode". The diagram in Fig. 2 is now familiar in a

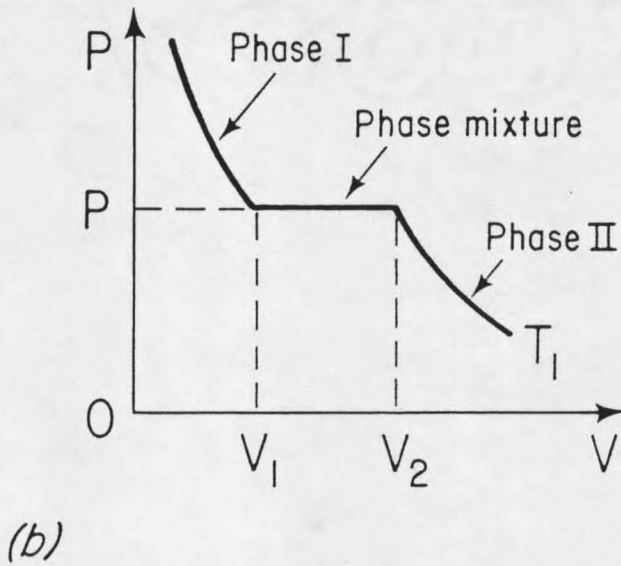
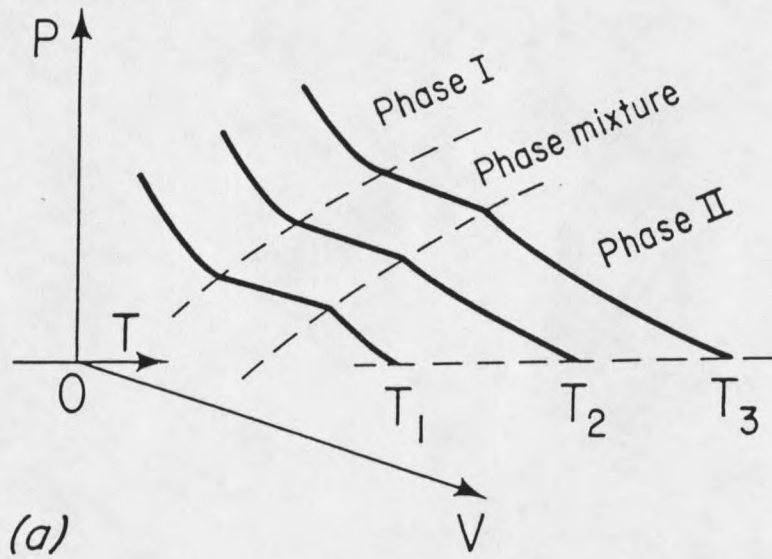


Fig. 1. Phase surface

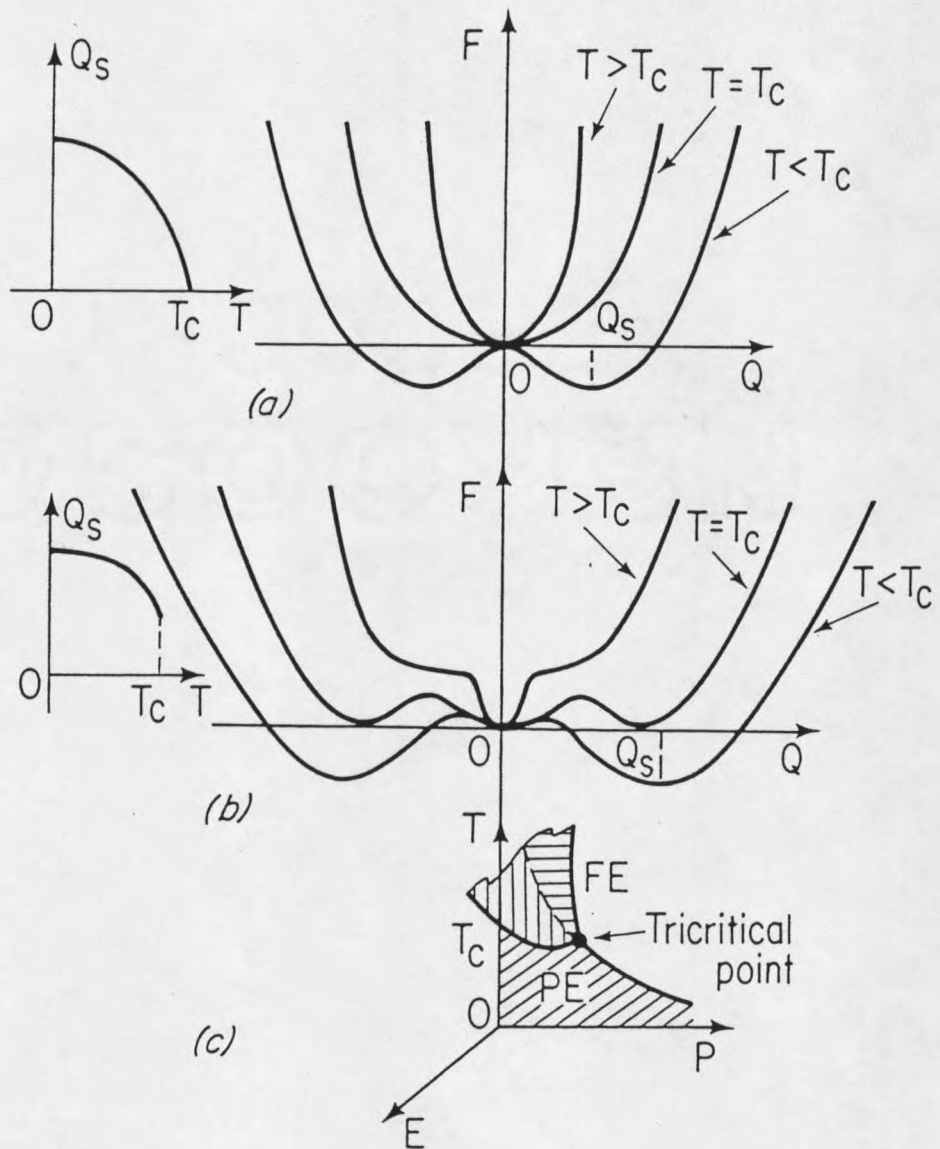


Fig. 2. Free energy and phase transition

variety of contexts. The free energy of a system is plotted versus a general displacement coordinate (order parameter) Q . Below a certain critical temperature T_c the lowest free energy state is obtained at nonzero values of Q . Depending on the sign of the quartic coefficient B in the free energy, the transition may be either continuous (second order) or discontinuous (first-order)². The value of Q which minimizes the free energy at a given temperature T is called the spontaneous value of the order parameter and is usually denoted $Q_s(T)$. Fig. 2(a) shows the dependence of the free energy on Q and T for a continuous transition (in which the quartic coefficient B in Eq.(I-1) is positive); the insert plots $Q_s(T)$ versus T for this case. Fig. 2(b) shows the dependence of free energy on Q and T for a discontinuous transition (in which the quartic coefficient B in Eq.(I-1) is negative); the insert plots $Q_s(T)$ versus T for this case. Fig. 2(c) shows second-order transitions as solid lines; first-order as dashed lines. The black dot is the tricritical point.³

The free energy used in this application is phenomenologically written as

$$F(Q, T) = A_0(T - T_0)Q^2 + BQ^4 + CQ^6 \quad \text{-----} \quad \text{(I-1)}$$

where $A_0(T - T_0)$ is a linear approximation for the quadratic coefficient which results from the mean field assumption

that all particles interact equally in the system; this is equivalent (Stanley 1971) to the assumption of interaction forces of infinite range, and is expected to be a good approximation for systems where Coulomb forces are dominant. The coefficient B is an explicit function of other variables, such as pressure p , applied electrical field E (for a ferroelectric), or stress S (for a ferroelastic). If $B(p)$ changes sign, a point (T_c, p_c) where the transition changes from second-order to first-order exists in (p, T) space. This is called a tricritical point, because in the three-dimensional T, p, E parameter space for a ferroelectric there are three lines of second-order phase transition boundaries which intersect at (T_c, p_c) . This is diagrammed in Fig. 2(c) (Scott, 1976). Such situations are well-known in ferroelectrics such as KH_2PO_4 and SbSI , and they have been studied in detail by light scattering by Peercy (1976).³ Gammon et al. found that at pressure near and above the tricritical pressure the Brillouin spectrum becomes strongly overdamped and narrower than 50 MHz, the width of the elastic peak in the best crystal.⁴ In the free energy expansion, there may be logarithmic terms which result from dipole-dipole interactions in a system, that is so-called logarithmic corrections.⁵ Free energy descriptions have been applied successfully in some steady-state systems. From the

point of view of statistical mechanics, a grand partition function, Z_G is given by

$$Z_G(z, V, T) = \sum_{N=0}^{\infty} z^N Z_N(V, T) \quad \text{-----} \quad (\text{I-2})$$

where N is number of a system, V is the volume, T is temperature, z is equal to $\exp(\mu/kT)$, where μ is its chemical potential, Z_N is the classical canonical partition function given by

$$Z_N(V, T) = (1/N\lambda^{3N}) \int \exp[-\Omega(\bar{r}_1, \bar{r}_2, \dots, \bar{r}_N)/kT] d^{3N}\bar{r} \quad (\text{I-3})$$

where λ , the thermal wavelength, is given by $\sqrt{h^2/(2\pi mkT)}$, and $\Omega(\bar{r}_1, \bar{r}_2, \dots, \bar{r}_N)$ is the potential energy of the system, which indicates all interactions among the particles. Obviously, the partition function

$$Z_G(z, V, T) \approx \sum_{N=0}^B z^N Z_N(V, T) \quad \text{-----} \quad (\text{I-4})$$

if B is large enough, and then

$$Z_G(z, V, T) \approx \pi(1-z/z_k) \sum_{N=0}^B \quad \text{-----} \quad (\text{I-5})$$

where z_k are the roots of the polynomial $\sum_{N=0}^B z^N Z_N(V, T)$.

Let z_0 be the value on the real axis corresponding to a

zero of $Z_G(z, V, T)$. At this point some thermodynamic variables or their derivatives may show discontinuities, when the volume V goes to infinity. This point is the phase transition point².

While the thermodynamic treatment of phase transitions is very fundamental and useful, it does not provide a geometrical picture of the microscopic changes accompanying a transition. The transitions accompanied by microscopic structural change are called structural phase transitions (SPT). The ferroelectric (FE) phase transitions are structural phase transitions. However, two categories, the displacive transition and order-disorder transition are generally classified⁶. Two limiting cases are known:

1) The crystal symmetry is lowered by a spontaneous displacement of sublattices against each other (displacive transition) or

2) Certain atoms or atomic groups have several positions (spatial or directional). In the disordered phase these positions are occupied at random, while in the ordered phase spontaneous ordering in one position takes place (order-disorder transition)⁷.

During the phase transition the physical properties of the material such as the dielectric constant or stiffness constant will change. For structural phase transitions we

must study not only the static but also the dynamic properties of the material such as the soft mode, frequency shift of the phonon, attenuation anomalies along with the dielectric constant for a ferroelectric material.

According to the well-known Lyddane-Sachs-Teller (LST) relation

$$\Omega_{L_0} / \Omega_{T_0} = \sqrt{\epsilon_s / \epsilon_\infty} \quad \text{-----} \quad \text{(I-6)}$$

where Ω_{L_0} is the frequency of the longitudinal optical mode, Ω_{T_0} is the frequency of the transverse optical mode. ϵ_s is the static dielectric constant while ϵ_∞ the infinite frequency dielectric constant corresponding to frequencies much higher than phonon frequencies, at which only the electrons contribute to the dielectric response⁸.

For some dielectric crystals, when $T=T_c$, ϵ_s goes to infinity and then Ω_{T_0} goes to zero.

Practically all experimental investigations deal with the order parameter, either measuring it directly or a generalized susceptibility, which describes its response in space and time. The pertinent experimental methods can be classified into two groups:

1) The system to be studied is exposed to an external influence and the response of the whole system is measured.

2) The variation of local properties is probed locally

within the system.

To the first group belong all the scattering experiments, where the external influence is, for example, a laser beam, x-rays or thermal neutrons and also measurement of material properties, such as the dielectric constant, refractive index, specific heat, etc.. By the method in the first category one determines a correlation of physical quantities.⁹

Examples for the second group are electron and nuclear magnetic resonance experiments.

With the introduction of lasers in the 1960's, light scattering spectroscopy was immediately transformed into a straightforward experimental technique. Raman scattering studies of the soft modes in KTaO_3 and SrTiO_3 were first reported by Fleury and Worlock (1967). Subsequently, Kaminow and Damen (1968) observed an overdamped soft mode in the Raman spectrum of KH_2PO_4 . Fleury et al. (1968) first demonstrated the utility of the soft mode concept for cell-multiplying phase transitions in their study of the cubic-tetragonal transition in SrTiO_3 . Similarly, Brillouin scattering (Mandelstam-Brillouin scattering in the Russian literature) was applied to the investigation of acoustic modes near phase transitions, complementing the earlier techniques of acoustic resonance and ultrasonic propagation. A soft acoustic mode in KH_2PO_4 ¹

was observed by Brillouin scattering by Brody and Cummins (1968).

Since 1970 the emphasis in light scattering of phase transitions has gradually shifted from simple soft mode analysis to aspects of spectra associated with mode coupling, central peaks, polarization coupling with the phonons, modification of the classical soft mode behavior due to critical fluctuations, etc..

The main activity in light scattering investigations of phase transitions concerns the spectrum of scattered light. The starting point of the theory of spectral anomalies is also the idea of the loss of stability, i.e., vanishing of restoring forces for a lattice distortion at the phase transition temperature. This leads to the condition that one of the lattice frequencies is expected to become zero at the phase transition, i.e., to the famous "soft mode" concept. This concept was developed primarily by Ginzburg (1949a, b), Cochran (1960, 1961) and Anderson (1960). There are several types of fluctuation responsible for the scattering. These different sources of scattering can be distinguished on the basis of their temporal behavior in the spectrum of the scattering light. In an insulating crystal the main source of scattering is dielectric constant modulation by acoustic lattice vibrations. Another source in crystals containing certain

atom groups (such as sarcosine) is the internal vibration modes of the molecular group. The optical vibrations of the lattice and the molecular vibrations are the source of what is called the vibrational Raman effect. The optical vibrations of the lattice and the molecular vibrations are of higher frequency. These vibrations result in spectral lines that are displaced from the incident light frequency by from about 50 to over 3500 cm^{-1} . The acoustic lattice vibrations which are much lower frequency for the small wavevectors involved in light scattering are the sources of the Brillouin spectrum, which usually is within 1 cm^{-1} from the incident light frequency. For acoustic modes each primitive cell acts as one mass point, so there are three acoustic modes or branches corresponding to the three degrees of freedom per particle. Thus the Brillouin spectrum will contain three sets of doublets symmetrically placed about the Rayleigh line. But often, the degeneracies in the acoustic branches and selection rules governing the scattered intensity reduce the number of observed Brillouin components. The longitudinal acoustic vibration mode alters the density of the sample and thus the dielectric constant. One predicts the intensity of the longitudinal Brillouin components to be stronger than the intensity of the transverse Brillouin components.

Now we can relate the observed Brillouin splitting, $\delta\Omega$,

to the incident light frequency, Ω_0 , and the scattering angle θ ; via the Brillouin relation

$$\delta\Omega/\Omega_0 = 2n(v/c) \sin(\theta/2) \quad \text{-----} \quad (\text{I-7})$$

where n is the refractive index of the scattering medium and c is the velocity of light in vacuum. Obviously, the Ω_0 is given (the laser frequency is known), and the refractive index n is given or can be measured and the scattering angle θ is determined by the experimental geometry. Thus we need only measure the Brillouin shift of the spectrum to determine the sound velocity of thermally excited acoustic lattice vibrations. This is the essence of the principle of Brillouin scattering.

We can consider the Brillouin scattering process as Bragg diffraction of the incident beam by the wave corresponding to some fluctuation. Even more simply, Brillouin scattering can be viewed as diffraction of incident light by gratings created by sound waves. For example, sound waves cause fluctuations of density, and thus of dielectric constant. These fluctuations act like a grating moving along the wavevector at the speed of sound, so the diffracted light suffers the Doppler shift.

Brillouin scattering was first observed by Gross¹⁰ in liquids and has been used to investigate the elastic properties of alkali halide crystals, quartz,

ferroelectric transitions and other crystals exhibiting other transitions.

For a given scattering wavevector (i. e. for a given scattering angle) there is also scattering produced by non-propagating diffusive fluctuations. The frequency of this scattering light is the same as the frequency of incident light. Fluctuations of the temperature and non-propagating density fluctuations are the sources of this elastic scattering.

For a liquid-gas or liquid-solid transition in the vicinity of the critical point there is a scattering peak produced by density fluctuation. These fluctuations cause critical opalescence, which was first explained by Von Smoluchowski and Einstein. The scattering intensity is related to density-density correlations. We can picture this scattering as caused by a lot of "islands" of liquid in the gas or "islands" of solid in the liquid, resulting from big fluctuations in the vicinity of the critical point,

Recent studies of this critical opalescence using laser light sources and light-beating spectroscopy have greatly increased our knowledge of such transitions.

Ginzburg suggests¹¹ that an enhanced scattering, similar to critical opalescence, should be observed in the vicinity of an order-disorder transition. This scattering

would be produced by large fluctuations in the degree of order. An enhanced scattering at the α - β transition in quartz was observed,¹² but it was shown to be due to a static twinning of the crystal.¹³

Because the ferroelectric-paraelectric transition is a structural phase transition, the measurement stated above may provide an indication of the presence of such a "critical opalescence" in the vicinity of the structural phase transition in Tris-Sarcosine Calcium Chloride (TSCC). Such an enhanced quasi-elastic scattering may be performed in the future.

The second reason for the present measurement is to investigate the high frequency sound velocities, the elastic constants, and the attenuation in both the paraelectric and ferroelectric phases. The criterion for deciding what is a high or lower frequency is the inverse of the response time of the order parameter, which is called the relaxation time.

Brillouin scattering measures phonon frequencies in the microwave region. These frequencies are higher than the inverse of the relaxation time for the order parameter. Thus, Brillouin scattering measurements can provide data on the magnitude of the dispersion in the longitudinal sound velocities in TSCC.

We have measured a temperature dependent dispersion in

the velocities of the longitudinal modes propagating along b and c crystal directions. We have done right angle scattering, small angle scattering and backscattering. The smallest angle we have achieved is 7.48° . The large frequency range that we worked on is about 2 GHz to 32 GHz. We have measured the natural line width of the longitudinal Brillouin components for temperatures from 300 K to 110 K. From these widths we determined the lifetime of the microwave frequency of sound waves in the 300 K-110 K temperature region. We also got the temperature dependence of the phonon life times.

From the temperature dependence of the velocities investigated in this work, we can also determine the temperature dependence of the three elastic constants of TSCC via the relation of the velocity to the elastic constant and density.

In Chapter II we present the theory of Brillouin scattering for crystals of orthorhombic structure such as TSCC. Chapter III presents the experimental technique and apparatus used in our experiment. Chapter IV presents the experimental results of our measurements of Brillouin spectra. Chapter V gives a discussion of these results in terms of the relaxation theory of sound absorption due to phonon-polarization coupling theory in TSCC. We interpret the anomalies of sound velocities and attenuations for

[001] phonons by pure piezoelectric coupling and for [010] phonons by piezoelectric coupling with small depolarization effect.

CHAPTER II

THEORY OF BRILLOUIN SCATTERING IN
ORTHORHOMBIC CRYSTAL

Introduction

In this chapter we will calculate the Brillouin spectrum from orthorhombic crystals in terms of the sound velocities, polarization, and the wavevector of the acoustic modes with respect to elastic constants and then calculate the intensity, polarization and frequency splitting of the Brillouin components for the scattering from acoustic modes propagating in the a, b, and b, c planes of an orthorhombic crystal. The complete theory of Brillouin scattering in cubic crystals has been given by Benedek and Fritsch.¹⁴ The general equations of their calculation are specialized to the case of scattering from acoustic modes propagating in the [110] planes. Nobody has yet provided the theory of Brillouin scattering in orthorhombic crystals. In this case the calculation will be more complicated than for a cubic crystal. Principal axes of the dielectric tensor are the crystal axes,

and the three elements are equal for cubic crystals, while for orthorhombic crystals the principal axes of the dielectric tensor are the crystal axes also, but the three elements are not equal. The stiffness tensor for orthorhombic crystals has more elements than for cubic crystals.

The Spectrum of the Scattering Field

Basically, the Brillouin scattering is a sort of radiation by the current and charge systems which are functions of time. We can expand these function in Fourier series. Thus we only need to deal with each Fourier component. We only consider the potential, field and radiation produced by finite systems of current and charge without losing generality.¹⁵

We assume

$$\rho(\bar{r}, t) = \rho(\bar{r}) e^{-i\Omega t}$$

$$\bar{J}(\bar{r}, t) = \bar{J}(\bar{r}) e^{-i\Omega t}$$

----- (II-1)

As usual the real parts of these functions are the physical quantities.

In the Lorentz gauge the vector potential is

$$\bar{A}(\bar{R}, t) = (1/c) \int d^3\bar{r}' \int dt' (\bar{J}(\bar{r}', t') / |\bar{R} - \bar{r}'|) \delta[t' + (|\bar{R} - \bar{r}'|/c) - t] \quad \text{-----} \quad (\text{II-2})$$

Substituting (II-1) into (II-2), we get

$$\bar{A}(\bar{R}) = (1/c) \int \bar{J}(\bar{r}) (e^{i k |\bar{R} - \bar{r}|} / |\bar{R} - \bar{r}|) d^3\bar{r} \quad \text{-----} \quad (\text{II-3})$$

where $k = \Omega/c$ and

$$\bar{A}(\bar{R}, t) = \bar{A}(\bar{R}) e^{-i \Omega t} \quad \text{-----} \quad (\text{II-4})$$

Then the magnetic field is

$$\bar{B} = \nabla \times \bar{A} \quad \text{-----} \quad (\text{II-5})$$

and the electric field outside the source is

$$\bar{E} = (i/k) \nabla \times \bar{B} = (i/k) \nabla \times (\nabla \times \bar{A}) \quad \text{-----} \quad (\text{II-6})$$

In principle, if the current distribution $\bar{J}(\bar{r})$ is given, we can calculate the field via the integral (II-3). There are three regions. Let the size of the source be d , the wave length λ , the distance from the origin to the position of observation R . The three regions are

near (static) region	$d \ll R \ll \lambda$
middle (induction) region	$d \ll R \approx \lambda$
far (radiation) region	$R \gg \lambda \gg d$

Here, we are only interested in the radiation region.

In this region as shown in Fig. 3, $kr \gg 1$ and e^{ikr} oscillates very fast. Then we can make the sufficiently accurate approximation

$$|\bar{R} - \bar{r}| \approx R - \bar{I} \cdot \bar{r} \quad \text{-----} \quad (\text{II-7})$$

where \bar{I} is the unit vector in the direction of \bar{R} and \bar{r} is the distance to the radiating point. Then the integral (II-3) becomes

$$\lim_{R \rightarrow \infty} \bar{A}(\bar{R}) = (e^{ikR}/cR) \int \bar{J}(\bar{r}) e^{-ik\bar{I} \cdot \bar{r}} d^3\bar{r} \quad - \quad (\text{II-8})$$

This means that in the far region, the vector potential is that of an expanding spherical wave with a factor which is a function of the solid angle. It is easy to show that the fields calculated from (II-5) and (II-6) are transverse to the radius vector and decrease as R^{-1} . They thus correspond to the radiation field. If the source dimensions are small compared to a wavelength it is appropriate to expand the integral in (II-8) in powers of k .

$$\lim_{kR \rightarrow \infty} \bar{A}(\bar{R}) = (e^{ikR}/cR) \sum [(-ik)^n/n!] \int \bar{J}(\bar{r}) (\bar{I} \cdot \bar{r})^n d^3\bar{r} \quad (\text{II-9})$$

If only the first term in (II-9) is kept, then the vector

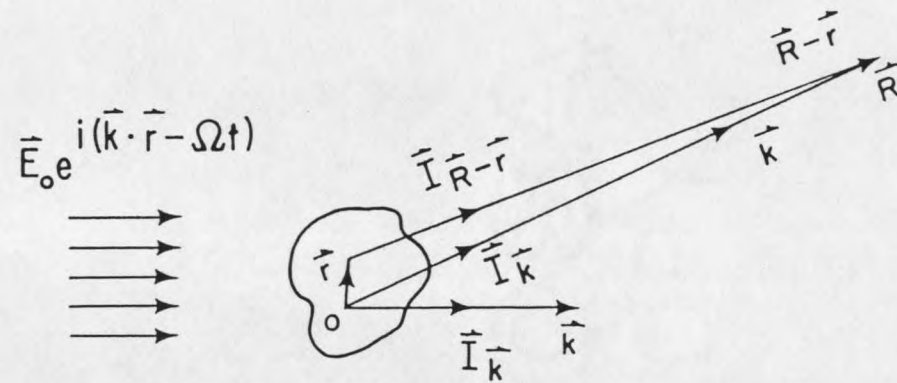


Fig. 3. Light scattering diagram

potential will be

$$\bar{A}(\bar{R}) = (e^{i\bar{k}\bar{R}}/cR) \int \bar{J}(\bar{r}) d^3\bar{r} \quad \text{-----} \quad (\text{II-10})$$

The integral can be put in more familiar terms by an integration by parts

$$\int \bar{J}(\bar{r}) d^3\bar{r} = - \int \bar{r}(\bar{\nabla}' \cdot \bar{J}) d^3\bar{r} + \bar{r} \cdot \bar{J} \Big|_{\infty}^0 \quad \text{-----} \quad (\text{II-11})$$

In the limit of large \bar{r} , $\bar{r} \cdot \bar{J} = 0$, so

$$\int \bar{J} d^3\bar{r} = -i\Omega \int \bar{r} \rho(\bar{r}) d^3\bar{r} \quad \text{-----} \quad (\text{II-12})$$

since from the continuity equation

$$i\Omega \rho(\bar{r}) = \bar{\nabla}' \cdot \bar{J} \quad \text{-----} \quad (\text{II-13})$$

Thus the vector potential is

$$\bar{A}(\bar{R}) = (-ike^{i\bar{k}\bar{R}}/R) \int \bar{P}(\bar{r}) d^3\bar{r} \quad \text{-----} \quad (\text{II-14})$$

where $\bar{P} = \rho(\bar{r}) \cdot \bar{r}$, the polarization.

Now we calculate the intensity and spectrum of light scattered from thermal fluctuations in liquids and solids. Since the media contain about 10^9 atoms in a region as small as the cube of the light wavelength, for a dimension of this order a liquid or solid may be regarded as a

continuum. A light wave passing through the medium produces an oscillating dipole moment per unit volume of polarization $\bar{P}(\bar{r}, t)$ at each point \bar{r} and at time t . The oscillating moments in turn radiate or scatter electromagnetic waves in all directions. From Equations (II-6) and (II-14), the electric field $d\bar{E}'$ at the field point \bar{R} caused by the oscillating dipole moments within a volume $|d^3\bar{r}| \ll \lambda^3$ is¹⁴

$$d\bar{E}'(\bar{R}, t) = [\bar{I}_{\bar{R}-\bar{r}} \times (\bar{I}_{\bar{R}-\bar{r}} \times d^2\bar{p}(\bar{r}, t') / dt^2) / c^2 | \bar{R}-\bar{r} |] d^3\bar{r} \quad \text{-----} \quad \text{(II-15)}$$

where the vectors \bar{R} , \bar{r} are the observation point outside the medium and the radiating point inside the medium. The unit vector \bar{I} is shown in Fig. 3.

If the radiation has low intensity, the local polarization is linearly proportional to the electric field. The proportional factor is a tensor α . It is convenient to decompose α into its time-average part $\langle \alpha \rangle$ and the time-space fluctuations $\delta\alpha(\bar{r}, t)$ produced by thermal fluctuations in the medium. In liquids and in cubic crystals the time-average polarizability $\langle \alpha \rangle$ is a scalar times the unity tensor and the index of refraction n is independent of the direction of propagation. However, the thermal fluctuation in a crystal causes off-diagonal components in the polarizability tensor, so we

should regard $\delta\alpha$ as a tensor whose elements fluctuate in time. Writing the electric field of the incident wave within the medium as

$$\bar{E}(\bar{r}, t) = \bar{E}_0 e^{i(\bar{k} \cdot \bar{r} - \Omega t)} \quad \text{-----} \quad (\text{II-16})$$

where $k = n\Omega/c$ is the wave vector of the light wave in the medium, we find that the polarization at each point in the medium is

$$\bar{p}(\bar{r}, t) = (\langle \alpha \rangle + \delta\alpha(\bar{r}, t)) \cdot \bar{E}_0 e^{i(\bar{k} \cdot \bar{r} - \Omega t)}$$

To calculate the second derivative of \bar{p} as required by Eq. (II-1), we have

$$\begin{aligned} d\bar{p}/dt &= -i\Omega_0 \langle \alpha \rangle \bar{E}_0 e^{i(\bar{k} \cdot \bar{r} - \Omega t)} - i\Omega_0 \delta\alpha \bar{E}_0 e^{i(\bar{k} \cdot \bar{r} - \Omega t)} \\ &\quad + [d(\delta\alpha)/dt] \bar{E}_0 e^{i(\bar{k} \cdot \bar{r} - \Omega t)} \quad \text{-----} \quad (\text{II-17}) \end{aligned}$$

$$\begin{aligned} d^2\bar{p}/dt^2 &= -\Omega_0^2 \langle \alpha \rangle \bar{E}_0 e^{i(\bar{k} \cdot \bar{r} - \Omega t)} - \Omega_0^2 \bar{E}_0 \delta\alpha e^{i(\bar{k} \cdot \bar{r} - \Omega t)} \\ &\quad - 2i\Omega_0 \bar{E}_0 e^{i(\bar{k} \cdot \bar{r} - \Omega t)} d(\delta\alpha)/dt \\ &\quad + [d^2(\delta\alpha)/dt^2] \bar{E}_0 e^{i(\bar{k} \cdot \bar{r} - \Omega t)} \quad \text{-----} \quad (\text{II-18}) \end{aligned}$$

We can see that the characteristic frequencies for

thermal fluctuations are small ($\leq 10^{12}$ Hz) compared to the light frequency in the optical region ($\approx 5 \cdot 10^{12}$ Hz). We may therefore keep just the first two terms in Eq. (2-18) and write

$$\begin{aligned} d^2 \bar{p}(\bar{r}, t) / dt^2 &\approx -\Omega^2 (\langle \alpha \rangle + \delta \alpha) \bar{E}_0 e^{i(\bar{k} \cdot \bar{r} - \Omega t)} \\ &= -\Omega^2 \bar{p}(\bar{r}, t) \end{aligned} \quad \text{-----} \quad \text{(II-19)}$$

On substituting Eqs. (II-19) and (II-18) into (II-15), (II-1) and carrying out the integration over the illuminated volume V at the retarded time t' , we find that if $\bar{R} \gg \bar{r}$

$$\begin{aligned} \bar{E}'(\bar{R}, t) &= [-(\Omega/c)^2 e^{i(\bar{k} \cdot \bar{R} - \Omega t)} / R] \cdot \bar{I}_k \times [\bar{I}_k \\ &\quad \times \int (\langle \alpha \rangle + \delta \alpha(\bar{r}, t)) \bar{E}_0 e^{i(\bar{k} \cdot \bar{r}' - \Omega t')} \cdot \bar{r}'] d^3 \bar{r}' \end{aligned} \quad \text{(II-20)}$$

where we have made use of the fact that if $\bar{R} \gg \bar{r}$,

$$\bar{I}_{\bar{R}-\bar{r}} \approx \bar{I}_k$$

and

$$n\Omega/c |\bar{R}-\bar{r}| \approx n\Omega/c \bar{I}_k \cdot (\bar{R}-\bar{r})$$

and

$$\bar{k}' = n\Omega\bar{I}_k / c$$

and

$$|\bar{R}-\bar{r}| \approx R$$

The integral (II-20) indicates the superposition of phases of waves scattered from each illuminated point in the crystal volume. If the fluctuation $\delta\alpha$ is absent, this superposition leads to a complete cancellation of the scattered waves. The contribution to the integral from the $\langle\alpha\rangle$ term is zero except in the forward direction. Scattering out of the incident direction results entirely from fluctuations in the polarizability.

By decomposing the fluctuations into their spatial Fourier components

$$\delta\alpha(\bar{r}, t') = (2\pi)^{-3/2} \int_{\mu} |dq| \delta\alpha(\bar{q}) e^{i[\bar{q}\cdot\bar{r} \pm \Omega_{\mu}(\bar{q}) t']} \quad \text{(II-21)}$$

where \bar{q} is the wavevector of the fluctuation and $\Omega_{\mu}(\bar{q})$ is the frequency of the fluctuation corresponding to this wavevector (wavelength). The superscript μ denotes the branch in the dispersion relation connecting \bar{q} and Ω . In general, $\Omega_{\mu}(\bar{q})$ can be complex to include a description of the damping of the fluctuations. $\Omega_{\mu}(\bar{q})$ is double valued

with \pm to account for the degeneracy in the dispersion relation for positive and negative running waves. We now can put Equation (II-21) into (II-20), being careful to include the effect of time retardation in $\delta\alpha$. We obtain

$$\begin{aligned} \bar{E}'(\bar{R}, t) &= -(\Omega/c)^2 \sum_{\mu} [e^{i(\bar{k}' \cdot \bar{R} - t)/R}] \bar{I}_k X [\bar{I}_k X] \int \int (2\pi)^{-3/2} \\ &\quad |dq| \delta\alpha_{\mu}(\bar{q}) e^{i(\bar{q} \cdot \bar{r} \pm \Omega_{\mu}(\bar{q})t)} \bar{E}_0 e^{i(\bar{k} - \bar{k}') \cdot \bar{r}} |d\bar{r}| \\ &= -(\Omega/c)^2 \sum_{\mu} e^{i(\bar{k}' \cdot \bar{R} - \Omega_{\mu}(\bar{q})t)/R} \bar{I}_k X \{ \bar{I}_k \\ &\quad X \int |dq| \delta\alpha_{\mu}(\bar{q}) e^{i[\bar{q} \cdot \bar{r} \pm \Omega_{\mu}(\bar{q})(t - \bar{I}_k \cdot (\bar{R} - \bar{r})/c_m)]} \\ &\quad \bar{E}_0 \int e^{i(\bar{k} - \bar{k}') \cdot \bar{r}} d^3\bar{r} \quad \text{-----} \quad \text{(II-22)} \end{aligned}$$

$$\begin{aligned} e^{i\bar{k}' \cdot \bar{R}} \cdot e^{-i\Omega_{\mu}/c_m \bar{I}_k \cdot \bar{R}} &= e^{i(\bar{k}' - \Omega_{\mu}/c_m \bar{I}_k) \cdot \bar{R}} \\ &= e^{i(\Omega/c \pm \Omega_{\mu}/c_m) \bar{I}_k \cdot \bar{R}} \\ &= e^{i((\Omega \pm \Omega_{\mu})/c_m) \bar{I}_k \cdot \bar{R}} \\ &= e^{i\bar{k} \cdot \bar{R}} \end{aligned}$$

where $\bar{k} = (\Omega \pm \Omega_{\mu}(\bar{q}))/c_m$

$$\begin{aligned} e^{i(\bar{q} \cdot \bar{r} \pm \Omega_{\mu}/c_m \bar{I}_k \cdot \bar{r})} e^{i(\bar{k} - \Omega/c_m \bar{I}_k \cdot \bar{r})} \\ &= e^{i(\bar{q} - (\Omega \pm \Omega_{\mu})/c_m \bar{I}_k - \bar{k}) \cdot \bar{r}} \\ &= e^{i(\bar{q} - \bar{k}' + \bar{k}) \cdot \bar{r}} \end{aligned}$$

Hence

$$\begin{aligned} \bar{E}'(\bar{R}, t) = & -(\Omega/c)^2 \sum_{\mu} \bar{I}_k x [\bar{I}_k x] |dq| \delta\alpha_{\mu}(\bar{q}) \cdot \bar{E}_0 \\ & \cdot (e^{i[\bar{k} \cdot \bar{R} - (\Omega \pm \Omega_{\mu}(\bar{q})) t]} / R) \\ & \cdot (2\pi)^{-3/2} \int |d\bar{r}| e^{i(\bar{k} - \bar{k}' + \bar{q}) \cdot \bar{r}} \quad (\text{II-23}) \end{aligned}$$

The final integral in Equation (II-23) is a delta function provided that the illuminated region is very large compared to the wavelength of light. In this case

$$\int e^{i(\bar{k} - \bar{k}' + \bar{q}) \cdot \bar{r}} |d\bar{r}| = (2\pi)^3 \delta[\bar{q} - (\bar{k}' - \bar{k})] \quad (\text{II-24})$$

Thus the wavevector of the fluctuation which produces the scattering in the direction \bar{k}' is that which satisfies the implicit equation

$$\bar{q} = \bar{k}' - \bar{k} = \bar{K} \quad \text{-----} \quad (\text{II-25})$$

We replace vector \bar{q} in Equation (II-25) by \bar{K} and call it the scattering vector. The vector \bar{K} in this Equation can be interpreted physically in two equivalent ways. In photon terminology, it implies the conservation of momentum among the incident photon \bar{k} , the scattered photon \bar{k}' and the scattering fluctuation \bar{K} . We notice the relation $\bar{k}' = (\Omega \pm \Omega_{\mu}(\bar{q})) / c$. The wavelength of the scattered light is different from that of the incident

light because the scattering fluctuation can add or subtract a quantum of energy $\pm h\Omega_\mu(\bar{K})$ to the incident photon. In classical terms, Equation (II-5) indicates that a spatially periodic fluctuation can modulate the polarizability and hence the phase of waves scattered from each point in such away as to exactly cancel out the phase factor $e^{i(\bar{k}' - \bar{k}) \cdot \bar{r}}$ produced by the combined effect of the spatial variation of the incident wave and the time retardation. As a result of this cancellation the radiation from each point in the medium adds coherently at the field point, or we can regard this phenomena as a Doppler effect. In this classical description, Equation (II-25) corresponds to a Bragg reflection of the light waves off the wave front of the fluctuation. We substitute Equations (II-25) and (II-24) into (2-23) and replace $\delta\alpha$ by $\delta\epsilon/4\pi$, where $\delta\epsilon$ is the fluctuation in the dielectric constant tensor. Obviously, $\bar{I}_R = \bar{I}_k$, so we relabel $\bar{E}'(\bar{R}, t) = \bar{E}(\bar{k}', t)$, (i.e. we emphasize the dependence of the scattered field on the direction of scattering)

$$\bar{E}'(\bar{R}, t) = \bar{E}(\bar{k}', t) = [-(\Omega/c)^2 (2\pi)^{3/2} / 4\pi R] \sum_{\mu} e^{i[\bar{k} \cdot \bar{R} - (\Omega \pm \Omega_{\mu}) t]} \cdot \bar{I}_k \times [\bar{I}_k \times (\delta\epsilon(\bar{K}) \cdot \bar{E}_0)] \quad \text{-----} \quad \text{(II-26)}$$

We can see from this equation there are three $\Omega_\mu(\bar{K})$ for the same wavevector \bar{K} . Thus in the spectrum there would

be three Brillouin scattering peaks.

The fluctuation of the dielectric constant is caused by the fluctuation of the lattice strain. The optical properties of crystals historically have been specified in terms of the indicatrix, and ellipsoid of resolution, the principal axes of which have length given by the inverse dielectric constants in the principal directions of the crystal. In more modern terms we may say that diagonalizes the dielectric tensor.

Equation (II-25) states that the scattering results from a particular Fourier component of the fluctuations in the dielectric constant. In the scattering process, momentum and energy are conserved. Momentum conservation relates the wavevectors of the incident wave \bar{k} , the scattered wave \bar{k}' and the scattering fluctuation \bar{K}

$$\hbar\bar{k}' = \hbar\bar{k} + \hbar\bar{K} \quad \text{-----} \quad (\text{II-27})$$

Energy conservation is indicated in the relationship between the incident light frequency Ω , the scattered light frequency Ω' and the frequency of the Fourier component of the fluctuation responsible for the scattering $\Omega_{\mu}(\bar{K})$

$$h\Omega' = h\Omega \pm h\Omega_{\mu}(\bar{K}) \quad \text{-----} \quad (\text{II-28})$$

where the \pm sign allows for scattering accompanied by

creation or annihilation of a phonon. These equations state that we are dealing with Bragg reflection of the incident light wave off the wavefront of the fluctuations for a particular wavevector \bar{K} . We can regard this scattering as the incident light being scattered by a moving one-dimensional periodic lattice. But since these fluctuations are propagating, the light frequency suffers a Doppler shift $\Omega \pm \Omega_\mu$.

We now calculate the magnitude of the wavevector of the fluctuation wave \bar{K}

$$|\bar{k}| = (n/c) (\Omega \pm \Omega_\mu)$$

$$\approx (n/c) \Omega. \quad \text{-----} \quad (\text{II-29})$$

because

$$\Omega_\mu \ll \Omega$$

and

$$|\bar{k}'| = n\Omega/c$$

$$|\bar{K}|^2 = k'^2 + k^2 - 2k'k \cos\theta$$

$$= (n_0 \Omega/c)^2 + (n^k \Omega/c)^2 - 2n^k n_0 \Omega^2 / c^2 \cos\theta$$

$$= (\Omega/c)^2 (n_0^2 + n^k{}^2 - 2n_0 n^k \cos\theta) \quad \text{--} \quad (\text{II-30})$$

$$|\bar{K}| = (\Omega/c) \sqrt{n_0^2 + n^k{}^2 - 2n_0 n^k \cos\theta} \quad \text{---} \quad (\text{II-30'})$$

If $n_o = n^k = n$

$$|\bar{K}| = (2\Omega n/c) \sin\theta \quad \text{-----} \quad (\text{II-31})$$

For small angle scattering $\theta \approx 0$ whether $n_o = n^k$ or not

$$\begin{aligned} |\bar{K}| &= (\Omega/c) \sqrt{n_o^2 + n_o^2 + 2n_o (dn/d\theta) \theta} \\ &\quad \text{-----} \\ &\quad - 2n_o (n_o + (dn/d\theta) \theta) \cos\theta \\ &= (\Omega/c) \sqrt{2n_o^2 - 2n_o^2 \cos\theta + (1 - \cos\theta) 2n_o (dn/d\theta) \theta} \\ &= (\Omega/c) \sqrt{2n_o^2 (1 - \cos\theta) + 2n_o (dn/d\theta) \theta (1 - \cos\theta)} \\ &= (2\Omega/c) \sqrt{n_o^2 + n_o (dn/d\theta) \theta \sin^2(\theta/2)} \\ &\approx (2\Omega/c n_o) \sin(\theta/2) \quad \text{-----} \quad (\text{II-32}) \end{aligned}$$

For anisotropic homogeneous material, the indicatrix has the following important properties. Draw through the origin a straight line OP in an arbitrary direction. Draw the central section of the indicatrix perpendicular to the line OP. This will be an ellipse. If the displacement \bar{D} of the wave propagating along OP is polarized in the direction of the semi-axis OA of the ellipse (i.e. \bar{D} vibrates parallel to OA), this has refractive index OA. If \bar{D} is parallel to OB (another semi-axis of the ellipse), then the wave has refractive index OB. Thus, only if the polarization of the light is along either OA

or OB, does the wave has a single refractive index shown in Fig. 4.

Assume the direction of the incident light is \bar{k} and polarization for \bar{E} inside the crystal is perpendicular to \bar{k} . The central section of the indicatrix perpendicular to \bar{k} must be an ellipse. If the semi-axes are OA and OB, the component of \bar{E} along OA and OB have refractive indices n_1 and n_2 respectively. The same relation holds for the scattered light. Each component of the incident light beam creates scattered light in the \bar{k}' direction. The scattered light itself has two components, with refractive indices, say, n_1' and n_2' . We may observe four phonons following the relations

$$k_1 = \Omega / c \sqrt{n_1^2 + n_1'^2}$$

$$k_2 = \Omega / c \sqrt{n_1^2 + n_2'^2}$$

$$k_3 = \Omega / c \sqrt{n_2^2 + n_1'^2}$$

$$k_4 = \Omega / c \sqrt{n_2^2 + n_2'^2} \quad \text{-----} \quad (\text{II-33})$$

If we do not distinguish the four waves, we can never measure the peak and particularly the lifetime of a given phonon. To obviate this problem, we have to find the optical axes and be very careful with the scattering geometry. Fortunately, TSCC is an orthorhombic structure

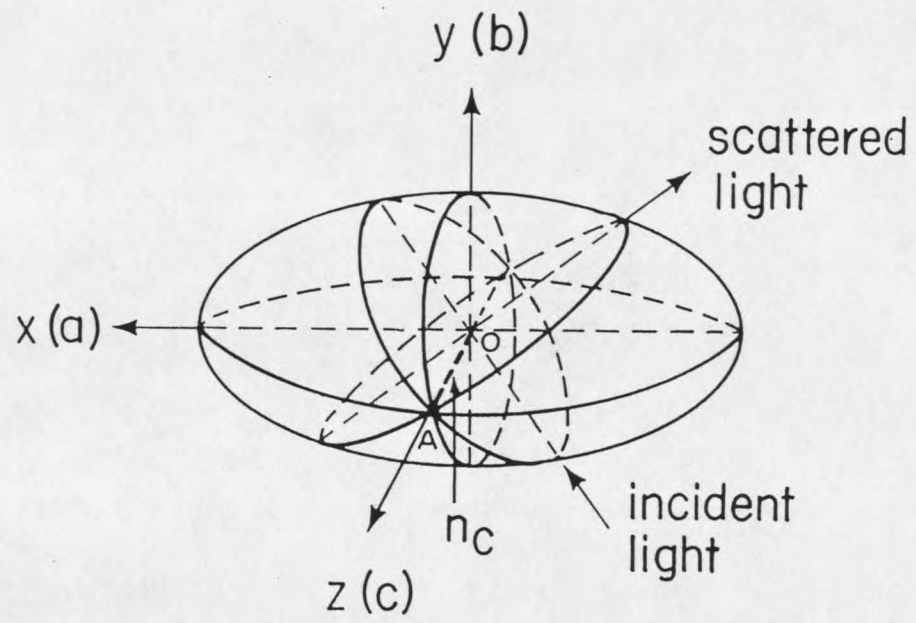


Fig. 4. Refractive indicatrix

for which the optical tensor axes lie along the crystal axes, and we are only interested in the longitudinal phonons. In this case the polarization of both the incident and scattered light is vertical, so that we don't worry about this problem.

The Fluctuation $\delta\epsilon$ of the Dielectric Constant

The refractive index of a crystal is specified by the indicatrix, which, as we have seen in section B, is an ellipsoid whose coefficients are the components of the refractive dielectric impermeability tensor B_{ij} for the optical axes, namely,

$$B_{ij}x_i x_j = 1 \quad \text{-----} \quad (\text{II-34})$$

and by the definition, $B_{ij} = k_0 dE_i / dD_j$, and $\epsilon_{ij} = dD_i / dE_j$, we have

$$\epsilon = 1/B$$

In general, a small change of refractive index, more precisely, a small change in the shape, size and orientation of the indicatrix, is produced by electric field and stresses. This change is most conveniently specified by giving the small change in the coefficients B_{ij} . If we neglect higher-order terms than the first in the fields and stresses, the changes of B_{ij} in the

coefficients under an applied field E_k and an applied strain ϵ_r , are given by

$$\delta B_{ij} = Z_{ijkl} E_k + p_{ijrs} \epsilon_r \quad \text{-----} \quad (\text{II-36})$$

In the Brillouin scattering, we only consider the second term, namely

$$\delta B_{ij} = p_{ijrs} \epsilon_r \quad \text{-----} \quad (\text{II-37})$$

or in another way

$$\delta B_m = p_{mn} \epsilon_n \quad (m, n=1, 2, 3, 4, 5, 6) \quad \text{---} \quad (\text{II-38})$$

Using the following conversion scheme

tensor notation	11	22	33	23, 32	31, 13	12, 21
matrix notation	1	2	3	4	5	6

The source of the fluctuation in $\bar{\epsilon}$ that interest us is the acoustic lattice vibrations or phonons. There are three such acoustic modes for each \bar{K} . These thermally excited lattice vibrations modulate the dielectric properties of the medium. This modulation occurs because the optical dielectric constant or refractive index is a function of the state of strain of the lattice. The optical properties of the crystal have been specified in terms of dielectric tensor ϵ_{ij} . In general, the fluctuation of the dielectric tensor can be expressed as

$$\delta\epsilon_{ij} = \sum p_{ijr} e_{rs} \quad \text{-----} \quad (\text{II-39})$$

where the ϵ_{rs} are the strain components which are defined in terms of the particle displacement u_i as

$$\epsilon_{rs}(\bar{r}, t) = (1/2) [du_r(\bar{r}, t)/dx_s + du_s/dx_r]$$

The indices r, s range over the values 1 to 3.

From Equation (II-20) we see that \bar{E}_0 can be taken outside the integral only if it does not change its direction. We assume the polarization of the incident light is along the optical axis. Thus for the outgoing light beam, we have two components in the direction of the two optical axes. The result for the intensity scattered into a unit solid angle in the direction \bar{K} is

$$\begin{aligned} dP_{\perp} / d\Omega &= P_0 n_{\perp} (\Omega/c)^4 [(2\pi)^3 / (4\pi)^2] \sum_{\mu=1}^3 [V / (2\pi)^3 \\ &\quad \cdot kT / 2\Omega_{\mu} (\bar{K})^2] | \bar{A}_{\perp} |^2 K^2 \\ &= P_0 (\Omega/c)^4 [V / (4\pi)^2] n_{\perp} \sum_{\mu=1}^3 | \bar{A}_{\perp} |^2 / (\rho v(\bar{K}, \Omega_{\mu})^2) \end{aligned} \quad \text{-----} \quad (\text{II-40})$$

$$\begin{aligned} dP_{\parallel} / d\Omega &= P_0 n_{\parallel} (\Omega/c)^4 [V / (4\pi)^2] \sum_{\mu=1}^3 | \bar{A}_{\parallel} |^2 / (\rho v(\bar{K}, \Omega_{\mu})^2) \end{aligned} \quad \text{-----} \quad (\text{II-41})$$

The temperature dependence comes from the kinetic energy of the phonon.

$$\begin{aligned}\langle E \rangle &= 2 \langle m \dot{u}^2 \rangle / 2 \\ &= 1 / [1 - e^{-h\nu / (kT)}] \\ &\approx kT/h\end{aligned}$$

The first form of (II-40) shows essential features of the intensity. The Ω^4 term is just the Rayleigh law, the parentheses include terms which are just the mean squared amplitude of the acoustic mode of frequency Ω propagating in the direction \bar{K} . The quantity $|\bar{A}_\mu|^2$ is the coupling constant that includes the selection rules and strength of the photoelastic coupling between the acoustic vibration and the dielectric constant. The K^2 term arises from the fact that the number of modes per unit frequency interval increases with K^2 .

We know that

$$\begin{aligned}\int \delta(\Omega) dK_x dK_y dK_z &= \int \delta(\Omega) 2\pi K^2 dK \\ &= \int \delta(\Omega) (2\pi K^2 / v) d\Omega \\ &= (2\pi / v^3) \int \delta(\Omega_\mu - \Omega_\mu) \Omega_\mu'^2 d\Omega_\mu' \\ &= (2\pi / v^3) (\Omega_\mu)^2 \quad \text{----} \quad \text{(II-42)}\end{aligned}$$

Substituting expression $\Omega_\mu = v(\bar{I}_k)K$, we get the second form of Equation (II-40). The summation over μ is a sum over the three acoustic branches, each of which has a polarization orthogonal to the other two branches.

We may thus expect the intensity

$$dP_\perp / d\Omega = P_0 n_\perp (\Omega/c)^4 (V/(4\pi)^2) \sum_{\mu=1}^3 |\bar{A}_\perp|^2 / [\rho v(\bar{K}, \Omega_\mu)^2]$$

$$\cdot \int (1/\pi) \{ \Gamma_\mu / [(\Omega' - \Omega \pm \Omega_\mu)^2 + \Gamma_\mu^2] \} d\Omega'$$

----- (II-40')

$$dP_\parallel / d\Omega = P_0 n_\parallel (\Omega/c)^4 (V/(4\pi)^2) \sum_{\mu=1}^3 |\bar{A}_\parallel|^2 / [\rho v(\bar{K}, \Omega_\mu)^2]$$

$$\cdot \int (1/\pi) \Gamma_\mu / [(\Omega' - \Omega \pm \Omega_\mu)^2 + \Gamma_\mu^2]$$

----- (II-41')

Here, we have included the fact that each Brillouin component has a width Γ_μ that arises from the finite lifetime of the phonons responsible for the scattering. The Lorentzian shape is a result of the assumption that phonons decay in time as $e^{-\Gamma t}$.

The \bar{A} determine the intensities of the Brillouin components and include the effects arising from the geometrical relationship of incident field polarization,

sound wave polarization and sound wave propagation direction. Explicitly

$$\bar{A} = \bar{I}_k \times \bar{I}_k \times \delta \bar{D} \quad \text{-----} \quad (\text{II-43})$$

where

$$\delta \bar{D} = \delta \epsilon \cdot \bar{E}_0 = \delta \epsilon \cdot E_0 \bar{I}_\epsilon \quad \text{-----} \quad (\text{II-44})$$

Acoustic Modes in a Monoclinic Crystal

To calculate the acoustic velocities and their dependence on propagation direction in the lattice we must solve the dynamical equation of motion

$$\rho d^2 u_i / dt^2 = \sum_j d \sigma_{ij} / dx_j \quad \text{-----} \quad (\text{II-45})$$

where u_i is the displacement in the i th direction, ρ is the density and σ_{ij} are elements of the stress tensor.

Now we choose coordinates for an orthorhombic crystal such as TSCC, such that x_1 is along a axis, x_2 along b and x_3 along c.

We treat the crystal in the long wavelength limit. We use the generalized Hooke's law to form the relation between the stresses and the strains.

$$\sigma_{ij} = \sum_{k,l} C_{ijkl} \epsilon_{kl} \quad \text{-----} \quad (\text{II-46})$$

Where the C_{ijkl} are the elastic constants of the crystal and e_{ki} are the elastic strain components defined before. Substituting e_{ki} into Equations (II-45) and (II-46) yields the wave equations

$$\rho d^2 u_i / dt^2 = \sum_{jkl} C_{ijkl} d^2 u_k / dx_j dx_l \quad \text{-----} \quad (\text{II-47})$$

We have used the symmetry property

$$C_{ijkl} = C_{ijlk}$$

and

$$C_{jikl} = C_{ijkl}$$

We seek plane wave solutions of Equation (II-47), having

$$\begin{aligned} u_i &= u_{i0} e^{i(\bar{K} \cdot \bar{r} - \omega t)} \\ &= u_{i0} e^{i(\Sigma K_x x - \omega t)} \quad \text{-----} \quad (\text{II-48}) \end{aligned}$$

Substituting Equation (II-48) into Equation (II-47),

we obtain

$$\rho \omega^2 u_i = \sum_{kj} C_{ikjl} u_k K_j K_l \quad \text{-----} \quad (\text{II-49})$$

Then

$$\begin{aligned} \rho \omega^2 u_i &= \sum_{kj} C_{1kjl} u_k K_j K_l + \sum_{kj} C_{2kjl} u_k K_j K_l + \sum_{kj} C_{3kjl} u_k K_j K_l \\ &= \sum_k C_{1k11} u_k K_1 K_1 + \sum_k C_{1k21} u_k K_2 K_1 + \sum_k C_{1k31} u_k K_3 K_1 \end{aligned}$$

$$\begin{aligned}
& + \sum_k C_{1k12} u_k K_1 K_2 + \sum_k C_{1k22} u_k K_2 K_2 + \sum_k C_{1k32} u_k K_3 K_2 \\
& + \sum_k C_{1k13} u_k K_1 K_3 + \sum_k C_{1k23} u_k K_2 K_3 + \sum_k C_{1k33} u_k K_3 K_3 \\
& = \sum_k (C_{1k11} K_1 K_1 + C_{1k21} K_2 K_1 + C_{1k31} K_3 K_1 + C_{1k12} K_1 K_2 \\
& + C_{1k22} K_2 K_2 + C_{1k32} K_3 K_2 + C_{1k13} K_1 K_3 + C_{1k23} K_2 K_3 \\
& + C_{1k33} K_3 K_3) u_k \quad \text{-----} \quad \text{(II-50)}
\end{aligned}$$

Here K_1, K_2, K_3 ($j, l=1, 2, 3$) are the components of \bar{K} along the crystal axes. Equation (II-50) becomes

$$\begin{aligned}
\rho \Omega^2 u_1 = & (C_{1111} K_1 K_1 + C_{1121} K_2 K_1 + C_{1131} K_3 K_1 + C_{1112} K_1 K_2 \\
& + C_{1122} K_2 K_2 + C_{1132} K_3 K_2 + C_{1113} K_1 K_3 + C_{1123} K_2 K_3 \\
& + C_{1133} K_3 K_3) u_1 + & (C_{1211} K_1 K_1 + C_{1221} K_2 K_1 \\
& + C_{1231} K_3 K_1 + C_{1212} K_1 K_2 + C_{1222} K_2 K_2 + C_{1232} K_3 K_2 \\
& + C_{1213} K_1 K_3 + C_{1223} K_2 K_3 + C_{1233} K_3 K_3) u_2 \\
& + & (C_{1311} K_1 K_1 + C_{1321} K_2 K_1 + C_{1331} K_3 K_1 + C_{1312} K_1 K_2 \\
& + C_{1322} K_2 K_2 + C_{1332} K_3 K_2 + C_{1313} K_1 K_3 + C_{1323} K_2 K_3 \\
& + C_{1333} K_3 K_3) u_3 \quad \text{-----} \quad \text{(II-51)}
\end{aligned}$$

We change from tensor to matrix notation, and obtain

